Proceedings of the Estonian Academy of Sciences,
2021, **70**, 4, 533–539
https://doi.org/10.3176/proc.2021.4.22
Available online at www.eap.ee/proceedings

MATERIALS
ENGINEERING

In-situ alloying of TiC-FeCr cermets in manganese vapour

Märt Kolnes*, Marek Tarraste, Jakob Kübarsepp, Kristjan Juhani and Mart Viljus

Department of Mechanical and Industrial Engineering, Tallinn University of Technology, Ehitajate tee 5, 19086 Tallinn, Estonia

Received 4 July 2021, accepted 26 July 2021, available online 12 November 2021

Abstract. Conventional vacuum sintering is, in general, inappropriate for producing manganese containing cermets because high vapour pressure combined with high sintering temperature of cermets (1400–1600 °C) causes considerable Mn loss through sublimation and evaporation. Sintering in Mn-rich microatmosphere does not only prevent Mn loss but also enables additional in-situ alloying of the binder phase during sintering. We studied alloying of TiC-based cermets bonded with high chromium steels, especially TiC-FeCr and TiC-FeCrMn, during sintering in Mn-rich atmosphere. Sintering in manganese vapour was detected to increase sinterability of the cermets, resulting in the formation of a ~1 mm thick Mn-rich surface layer with homogeneous microstructure while the core region of the material remained unaffected. This surface region of sintered TiC-FeCr and TiC-FeCrMn cermets exhibited increased Mn content and competitive mechanical properties – hardness of ~1150 HV30 and indentation fracture toughness of ~12 MPa·m$^{1/2}$.

Key words: TiC cermets, alternative binder, sintering environment.

1. INTRODUCTION

The most common ceramic-based composites are hardmetals where tungsten carbide grains are cemented in tough metal matrix. Primarily cobalt and nickel are used as main metal constituents (binders) in hardmetals. However, tungsten and cobalt as elements of high economic importance are in the list of critical raw materials in the world, especially in Europe [1]. Additionally, cobalt and nickel are toxic for humans [2]. As a result, research of partially or completely Co- and Ni-free ceramic-metallic composites with alternative binders, in particular WC-based hardmetals and W-free TiC(N)-based cermets, has intensified substantially during the last decades [3,4].

Austenitic-martensitic iron alloys with relatively high manganese concentrations (~13 wt%) are known for their toughness and wear resistance. This, coupled with the fact that FeMn alloys are less expensive, relatively abundant and non-toxic, makes them promising candidates for replacing Co- and Ni-based binder systems in ceramic-metallic composites (hardmetals and cermets). There have been attempts to develop wear resistant high-manganese WC-FeMn or WC-FeCrMn hardmetals [5–12] and W-free TiC-FeMn or TiC-FeCrMn [13–21] cermets. However, only few studies have directed attention to the fact that due to its high vapour pressure Mn is highly volatile at higher temperatures causing severe Mn loss through sublimation evaporation during vacuum sintering [6–9, 12,20,21].

Final consolidation of cermets takes place during liquid phase sintering at temperatures between 1300 and 1500 °C where the loss of elements with high vapour pressure intensifies [22]. Therefore, suitable methods must be employed to maintain high Mn content in the as-sintered materials. Although sintering in high vacuum is usually preferred and demonstrates superior oxide reduction, it is not suitable for Mn or Cr containing alloys because of aforementioned high vapour pressure. Lower sintering temperature and argon or nitrogen partial pressure can restrict the losses through sublimation and

* Corresponding author, mart.kolnes1@taltech.ee

evaporation. Mn losses can be further minimised by creating Mn vapour "microatmosphere". Schubert et al. showed that under optimised conditions up to 16 wt% Mn remained in the binder of WC-FeMn hardmetal [6]. Also, our previous research has proved that sintering of WC-FeMn and WC-FeCrMn hardmetals in Mn-rich "microatmosphere" facilitates not only maintaining, but even increases Mn content in as-sintered ceramic-metal composites [12].

Alloying of powder metallurgy materials in Mn-rich sintering atmosphere has also been addressed by other researchers, in particular by Šalak et. al. [23]. The study demonstrates uniformly alloyed surface layers of powder compacts formed as a result of condensation of manganese vapour combined with high-rate surface diffusion. Manganese vapour treatment for alloying is also used for platinum group metals [24].

The present research discusses structure formation, phase composition and mechanical performance of TiC-based cermets bonded with high-chromium corrosion resistant FeCr and FeCrMn binders alloyed in-situ in Mn-rich atmosphere.

2. EXPERIMENTAL DETAILS

TiC-FeCr(Mn) ceramic-metal composite powder mixtures with 70 wt% (78 vol%) of hard phase (nominal, calculated value) were produced using a conventional powder metallurgy routine. Two cermet grades were prepared:

(a) 70 wt% TiC and 30 wt% steel AISI430L powders were precursors for TiC-FeCr;
(b) 70 wt% TiC, 22.8 wt% steel AISI446, 6 wt% Mn and 1.2 wt% Si powders were precursors for TiC-FeCrMn.

The preparation of the powder mixtures was carried out in a ball mill (milling duration – 72 h; medium – isopropyl alcohol; WC-Co balls; 10:1 ball-to-powder weight ratio). The chemical composition, impurities, average particle size and the producer of starting powders are presented in Table 1.

Paraffin wax was added to the powder mixture as compacting aid and green samples were prepared employing uniaxial pressing. In-situ alloying sintering was carried out in the vacuum furnace (Red Devil, R. D. Webb Company Inc.) using a specially designed chamber for the generation of manganese vapour "microatmosphere" during sintering (see Fig. 1) [6]. The heating rate, maximum sintering temperature and holding time were 10 °C·min^{-1}, 1400 °C and 30 min, respectively. The cross-sections of sintered specimens were prepared (ground and polished) for characterization. The scanning electron microscope (SEM) Zeiss EVO MA15 equipped with the X-ray spectroscopy (EDS) system INCA was employed for microstructural and elemental composition analysis.

Phase composition was analysed with Rigaku SmartLab using Cu Kα radiation and the step size of 0.02°. Vickers hardness and microhardness were measured with Indentec 5030 KV (load 294.2 N) and Micromet 2001 (load 1 N), respectively. The indentation fracture toughness (K_{IC}) was measured by the Palmqvist method and the equation described in [25], (Eq. 1):

$$K_{IC} = 0.16 \times \left(\frac{c}{a}\right)^{-1.5} \times \left(H \times a^{\frac{1}{2}}\right), \quad (1)$$

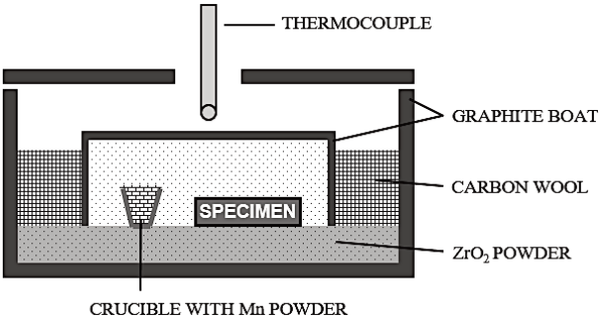

Fig. 1. Schematic build-up of the graphite crucible which includes the manganese vapour "microatmosphere".

Table 1. Description of starting powders

Powder	Chemical composition, wt%		Particle size, μm	Producer
	Basic components	Impurities		
TiC	C_{comb} – 19.12; Ti – bal.	O – 0.30; N – 0.02	2–4	PPM Ltd.
AISI430L (X2Cr17)	Cr – 16.8; Mn – 0.69; Si – 0.64; Fe – bal.	C – 0.02; P – 0.01; S – 0.01	10–45	Sandvik Osprey Ltd.
AISI446 (X18CrN28)	Cr – 24.2; Mn – 1.2; Si – 0.85; Fe – bal.	N – 0.25; C – 0.03; P – 0.011; S – 0.008	10–45	Sandvik Osprey Ltd.
Mn	Mn – 99.84	O – rest	7.95	PPM Ltd.
Si	Si – 99.50	Al – 0.15; Ti – 0.002; Fe – 0.2; P – 0.004; Ca – 0.05; B – 0.0005	44	Whole Win, Materials Sci. & Tech.

where c is the average length of the cracks emanating from the tips of the Vickers indentations (μm); a denotes the half length of the diagonal of Vickers indentations (μm); H represents Vickers hardness (MPa).

3. RESULTS AND DISCUSSION

Table 2 demonstrates the nominal chemical composition of TiC-FeCr and TiC-FeCrMn cermets before milling (calculated) and after sintering (EDS elemental analysis). The small fraction of tungsten in the sintered specimens is caused by the wear of WC-Co milling balls.

Therefore, based on weight change of the balls, the approximate tungsten content was also calculated. EDS analysis was performed from the cross-section of the sintered samples near the surface and from the core (central) region. Chromium and particularly manganese content in the surface region of vacuum sintered TiC-FeCr and TiC-FeCrMn cermets decreased considerably. The vacuum level during the conventional vacuum sintering was approximately 0.2–0.8 mbar, which caused reduction of chromium and considerable decrease in manganese content due to the sublimation and evaporation of these elements. During alloying sintering in the Mn-rich environment the manganese content increased drastically in the surface layer of both cermets. The mass loss caused by the removal of the paraffin wax was subtracted from the results. It correlates with the change in weight – the mass decrease of vacuum sintered cermets was 3.1 and 6.5 wt% while the mass increase after alloying sintering was 8.3 and 3.5 wt% in the case of TiC-FeCr and TiC-FeCrMn, respectively. However, the Mn content of the core of the material did not change much compared to the nominal chemical composition for both investigated cermets. This demonstrates that Mn losses can be prevented by creating a manganese vapour microatmosphere and manganese vapour in the sintering device has an alloying effect, however, only in the surface layers of the cermets.

Such a result is different from the previous research where WC-based hardmetals bonded with FeMn-based binders were prepared also via sintering in Mn-rich microatmosphere [12]. Sintering of WC-FeMn and WC-FeCrMn hardmetals facilitated not only maintaining but increased Mn content in surface as well as in central (core) regions of as-sintered composites. The difference in the results of the present research (TiC-based cermets) and previous research (WC-based hardmetals) may be

Table 2. Chemical composition and weight change of TiC-FeCr and TiC-FeCrMn cermets

				Chemical composition, wt%							Weight change**
				Ti*	C*	Fe	Cr	Mn	Si	W*	
TiC-FeCr	Calculated, after milling		Total	53.94	12.7	23.43	4.78	0.2	0.19	4.76	–
			Binder	–	–	81.92	16.71	0.70	0.66	–	
	Vacuum sintering	Surface layer	Total	63.06	15.02	14.22	3.09	0.12	–	4.49	–3.1%
			Binder	–	–	91.96	6.34	0.5	1.2	–	
		Core	Total	59.26	14.44	17.91	4.2	0.11	–	4.08	
			Binder	–	–	92.97	5.41	0.65	0.98	–	
	Alloying sintering	Surface layer	Total	40.56	12.87	26.67	5.58	**10.97**	–	3.35	8.3%
			Binder	–	–	67.58	6.22	**25.47**	0.73	–	
		Core	Total	58.84	13.96	18.42	4.35	0.19	–	4.24	
			Binder	–	–	91.95	6.18	0.91	0.96	–	
TiC-FeCrMn	Calculated		Total	53.94	12.88	16.09	5.27	5.77	1.29	4.76	–
			Binder	–	–	56.62	18.54	20.30	4.54	–	
	Vacuum sintering	Surface layer	Total	63.59	14.42	11.44	3.48	1.7	0.65	4.72	–6.5%
			Binder	–	–	77.21	6.39	9.76	6.65	–	
		Core	Total	57	13.27	15.07	4.64	4.56	0.7	4.77	
			Binder	–	–	71.07	5.34	17.68	5.91	–	
	Alloying sintering	Surface layer	Total	51.3	13.58	14.68	4.71	**10.82**	0.78	4.13	3.5%
			Binder	–	–	54.90	4.89	**35.20**	5.02	–	
		Core	Total	54.47	13.23	16.03	5.57	5.23	0.69	4.6	
			Binder	–	–	70.61	5.29	17.97	6.14	–	

* Although a small Ti, C and W signal was detected in the binder as well, the assumption was made that the majority of it comes from nearby TiC grains and not from the binder. Thus, the sintered binder composition was recalculated while excluding Ti, C and W.

** Weight change that occurs because the debinding (removal of paraffin wax during sintering) is excluded.

attributed to the substantial difference in sintering temperatures – WC-FeMn and WC-FeCrMn hardmetals were sintered at ~200 °C lower temperature compared with TiC-FeCr and TiC-FeCrMn cermets. The cross-section of TiC-FeCr cermet was further examined since the increase of Mn content in the surface layers as the result of sintering in Mn-rich atmosphere was most prominent. The EDS line-scan and microhardness measurements revealed that the thickness of the distinctive surface layer is about 1 mm (Fig. 2). The sublimation of manganese and formation of manganese vapour starts already at temperatures around 900–1000 °C [22]. The major densification of TiC-FeCr and TiC-FeCrMn cermets does not occur earlier than the formation of the liquid phase at sintering temperatures around 1300 °C. Despite the fact that open porosity and manganese vapour coexist, alloying of the specimen core does not occur during solid-state sintering (see Table 2). The SEM images of visually two-phase microstructures of TiC-FeCr cermets (darker TiC grains embedded in a brighter binder) after vacuum sintering and alloying sintering in Mn-rich atmosphere are presented in Figs 3 and 4, respectively. As can be seen, the whole cross-section of the vacuum sintered cermet and the core of the alloyed sintered cermet is characterised by an uneven distribution of the binder phase (binder pools) and residual porosity. Still, TiC-FeCrMn cermet exhibits slightly more uniform microstructure (Fig. 4). The modest sinterability is caused by insufficient reduction of oxides and incomplete wettability. In the case of vacuum sintering, the TiC-FeCr cermet requires temperatures about 1475 °C or alloying by strong carbide forming elements for developing a uniform microstructure with low porosity [26]. However, the distribution of the binder phase in the surface layer of the sintered cermets

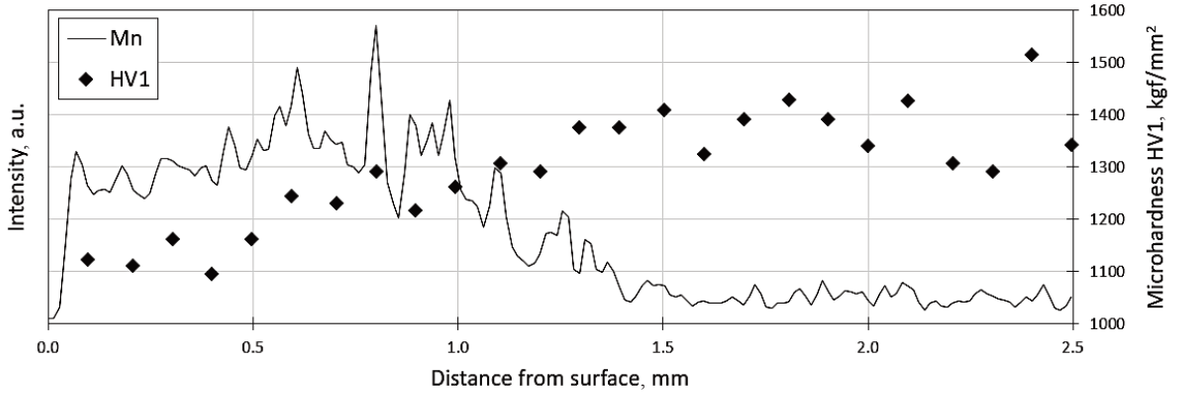

Fig. 2. The surface layer Mn content and microhardness profiles of TiC-FeCr cermet after alloying sintering in Mn-rich microatmosphere.

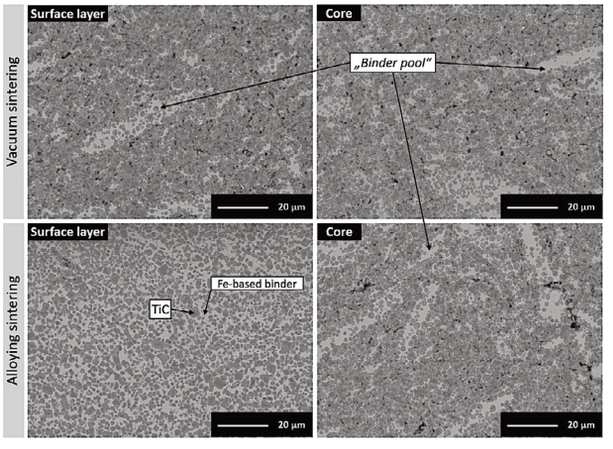

Fig. 3. The SEM images of microstructures of TiC-FeCr cermet after vacuum sintering (top) and alloying sintering in Mn microatmosphere (bottom). Microstructures of the surface layer (left) and the core region (right) are presented.

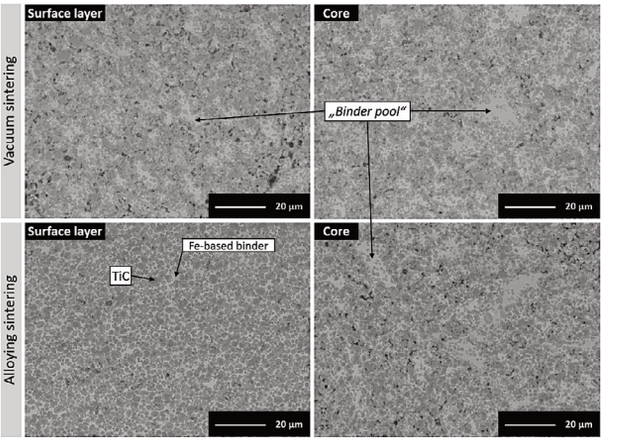

Fig. 4. The SEM images of microstructures of TiC-FeCrMn cermet after vacuum sintering (top) and alloying sintering in Mn microatmosphere (bottom). Microstructures of the surface layer (left) and the core region (right) are presented.

improves significantly during alloying sintering at 1400 °C in manganese microatmosphere – the microstructure is homogeneous and the porosity is decreased. It is the result of high deoxidation ability of manganese influencing the densification – it improves wetting conditions between the solid carbide grains and the liquid metallic binder phase. Despite the fact that Mn is present in the initial composition of TiC-FeCrMn powder mixture, the manganese vapour itself has a major positive effect on the improvement of structural homogeneity.

The mechanical properties (macrohardness and indentation fracture toughness (IFT)) were measured only from the regions with the desirable homogeneous microstructure – surface layers of the TiC-FeCr and TiC-FeCrMn cermets sintered in Mn-rich environment. Both cermets yielded relatively similar results with the hardness being in the range of 1100–1200 HV30 and IFT in the range of 11.5–12.5 MPa·m$^{1/2}$. These properties are comparable with the studies of other researchers [3]. Microhardness results showed that, as expected, the hardness measured in the central (core) region tends to fluctuate considerably (Fig. 2). This is due to the uneven phase distribution that characterises these regions of the prepared cermets.

X-ray diffraction (XRD) patterns of TiC-FeCr and TiC-FeCrMn cermets after alloying sintering in Mn-rich atmosphere are presented in Fig. 5. XRD analysis showed that the phase compositions of core and surface regions of TiC-FeCr cermet are dissimilar. As expected, the core region is composed of three phases. TiC, ferrite (α-Fe) and chromium-based mixed carbide (Cr, Fe)$_7$C$_3$. Interestingly, regardless of high Mn content in the surface layer (see Table 2), the ε-type hexagonal martensite was observed instead of austenite (γ-Fe). This result indicates that in the region that was alloyed with Mn via sintering in Mn-rich atmosphere, γ→ε martensitic transformation took place during cooling. The resulting metallic binder was ferritic-martensitic. The phase composition of the central and surface region of TiC-FeCrMn cermet is similar. Both regions comprise four phases: TiC, ferrite (α-Fe), chromium-based mixed carbide (Cr, Fe)$_7$C$_3$ and, as distinct from TiC-FeCr cermet, additionally austenite (γ-Fe). The formation of γ-Fe can be explained by high concentration of an austenite stabilising element – manganese.

The reason why the alloying with Mn vapour favoured the martensitic transformation, as opposed to the introduction of Mn in the initial powder mixture, needs further research. In addition, it is clear that achieving TiC-FeCrMn cermets with a fully austenitic binder is a challenging task – even at very high manganese concentrations the ferrite (α-Fe) is the dominant metallic phase.

4. CONCLUSIONS

TiC cermets bonded with high-chromium corrosion resistant steels were prepared using conventional vacuum sintering and sintering in Mn-rich environment (Mn "micro-atmosphere"). The microstructure analysis, energy dispersive X-ray spectroscopy, X-ray diffraction and mech- anical testing led to the following conclusions:

– Sintering of TiC-FeCr and TiC-FeCrMn cermets in Mn-rich microatmosphere does not only prevent Mn losses but also enables to increase Mn content in as-sintered composites.

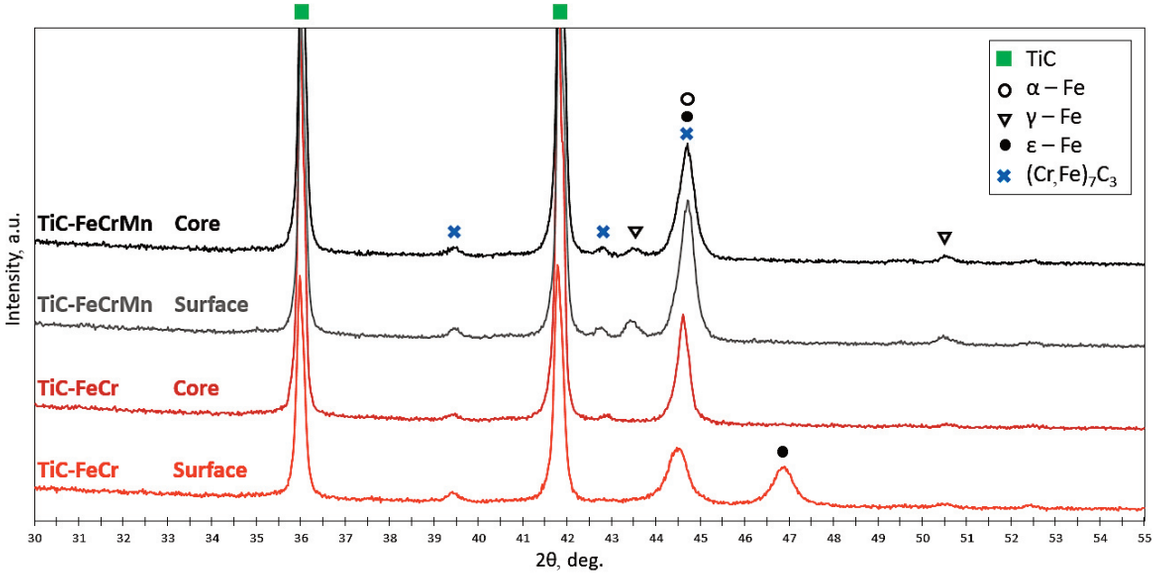

Fig. 5. X-ray diffractograms of the central (core) region and the surface layer of TiC-FeCr and TiC-FeCrMn cermets sintered in Mn-rich atmosphere.

– Regardless of open porosity before the formation of the liquid phase, the alloying effect was achieved only in the surface layer of the cermets with thickness of about 1 mm. Chemical composition and microstructure of the central (core) region remained largely unaffected by alloying sintering.
– Sintering in Mn-rich atmosphere has a substantial effect on the microstructure and phase composition of the surface regions of TiC-based cermets, in particular favouring densification and microstructure homogenisation, which in turn yielded satisfactory mechanical properties.

ACKNOWLEDGEMENTS

The research was supported by the Estonian Research Council grants PRG665 and PRG1145. The publication costs of this article were covered by the Estonian Academy of Sciences and Tallinn University of Technology.

REFERENCES

1. European Commission homepage. List of Critical Raw Materials for the EU. https://ec.europa.eu (accessed 2021-06-15).
2. REACH homepage. http://echa.europa.eu (accessed 2021-06-20).
3. Kübarsepp, J. and Juhani, K. Cermets with Fe-alloy binder: A review. *Int. J. Refract. Met. Hard Mater.*, 2020, **92**, 105290.
4. Norgren, S., García, J., Blomqvist, A. and Yin, L. Trends in the P/M hard metal industry. *Int. J. Refract. Met. Hard Mater.*, 2015, **48**, 31–45.
5. Murdoch, H. A. and Darling, K. A. Metric mapping: A color coded atlas for guiding rapid development of novel cermets and its application to "green" WC binder. *Mater. Des.*, 2018, **150**, 64–74.
6. Schubert, W. D., Fugger, M., Wittman, B. and Useldinger, R. Aspects of sintering of cemented carbides with Fe-based binders. *Int. J. Refract. Met. Hard Mater.*, 2015, **49**(1), 110–123.
7. Maccio, M. R. and Berns, H. Sintered hardmetals with iron–manganese binder. *Powder Metall.*, 2011, **55**(2), 101–109.
8. Hanyaloglu, C., Aksakal, B. and Bolton, J. D. Production and indentation analysis of WC/Fe–Mn as an alternative to cobalt-bonded hardmetals. *Mater. Charact.*, 2001, **47**(3–4), 315–322.
9. Hanyaloglu, S. C., Aksakal, B. and Şen, S. An indentation and stress analysis of WC/Fe-Mn hardmetals. *Indian J. Eng. Mater. Sci.*, 2003, **10**, 229–235.
10. Sevostyanova, I. N., Savchenko, N. L. and Kulkov, S. N. Structural and phase binder state and behavior during friction of WC-(Fe-Mn-C) composites. *J. Frict. Wear*, 2010, **31**(4), 281–287.
11. Siemiaszko, D., Rosinski, M. and Michalski, A. Nanocrystalline WC with non-toxic Fe-Mn binder. *Phys. Status Solidi C*, 2010, **7**(5), 1376–1379.
12. Tarraste, M., Kübarsepp, J., Juhani, K., Kolnes, M., Viljus, M. and Mere, A. Sintering of high Mn cemented carbides in Mn-rich environment. *Defect Diffus. Forum*, 2020, **405**, 402–407.
13. Li, G., Zhou, H., Lu, J., Wu, N., Lyu, Y. and Luo, F. TiC-high Mn steel-bonded cermets with improved strength and impact toughness. *Steel Res. Int.*, 2021, **92**(3), 2000400.
14. Li, G., Zhou, H., Yang, H., Huang, M., Peng, Y. and Luo, F. The preparation process, microstructure and properties of cellular TiC-high Mn steel-bonded carbide. *Materials*, 2020, **13**(3), 757.
15. Li, G., Jia, J., Lyu, Y., Zhao, J., Lu, J., Li, Y. and Luo, F. Effect of Mo addition mode on the microstructure and mechanical properties of TiC-high Mn steel cermets. *Ceram. Int.*, 2020, **46**(5), 5745–5752.
16. Li, G., Yang, H., Lyu, Y., Zhou., H. and Luo, F. Effect of Fe-Mo-Cr pre-alloyed powder on the microstructure and mechanical properties of TiC-high-Mn-steel cermet. *Int. J. Refract. Met. Hard Mater.*, 2019, **84**, 105031.
17. Li, H. W., Li, G. P., Guo, L. B., Luo, F. H., Wang, X. B. and Wang, S. T. Effect of WC additive on microstructural evolution and properties of TiC steel-bonded carbide. *Mater. Sci. Forum*, 2018, **913**, 453–458.
18. Wang, Z., Lin, T., He, X., Shao, H., Zheng, J. and Qu, X. Microstructure and properties of TiC-high manganese steel cermet prepared by different sintering processes. *J. Alloys Compd.*, 2015, **650**, 918–924.
19. Rong, S. F., Liu, C., Guo, J. W., Wang, M. X. and Liu, Q. L. The influence of Hadifield steel-bonded TiC preparation process on microstructure and properties. *Adv. Mat. Res.*, 2011, **291**–**294**, 1825–1830.
20. Kolnes, M., Kübarsepp, J., Kollo, L. and Viljus, M. Characterization of TiC-FeCrMn cermets produced by powder metallurgy method. *Mater. Sci. (Medžiagotyra)*, 2015, **21**(3), 353–357.
21. Kolnes, M., Kübarsepp, J., Viljus, M., Traksmaa, R. and Illopmägi S. Effect of sintering conditions on microstructure and performance of TiC-FeCrMn cermets. In *Proceedings of the World PM2016 Congress*, *Hamburg, Germany, October 9–13, 2016*. EPMA.
22. Tadashi, M. (ed.). *Application of Thermodynamics to Biological and Materials Science*. IntechOpen, London, 2011.
23. Šalak, A. and Selecká, M. *Manganese in Powder Metallurgy Steels.* Springer, New York, NY, 2012.
24. Taninouchi, Y. and Okabe, T. H. Vapor treatment for alloying and magnetizing platinum group metals. In *Rare Metal Technology 2017* (Kim, H., Alam, S., Neelameggham, N., Oosterhof, H., Ouchi, T. and Guan, X., eds). Springer, Cham, 2017, 119–127.
25. Evans, A. G. and Charles, E. A. Fracture toughness determinations by indentation. *J. Am. Ceram. Soc.*, 1976, **59**(7–8), 371–372.
26. Kolnes, M., Mere, A., Kübarsepp, J., Viljus, M., Maaten, B. and Tarraste, M. Microstructure evolution of TiC cermets with ferritic AISI 430L steel binder. *Powder Metall.*, 2018, **61**(3), 197–209.

Titaankarbiidkermiste *in situ* legeerimine mangaani aurus

Märt Kolnes, Marek Tarraste, Jakob Kübarsepp, Kristjan Juhani ja Mart Viljus

Käesolevas töös uuriti titaankarbiidi baasil kermiseid, mille sideaine on suure kroomisisaldusega korrosioonikindel teras. Kermiste valmistamisel kasutati tavalist vaakumpaagutust ja paagutamist mangaanirikkas keskkonnas (mangaani mikroatmosfääris). Vaakumkeskkonnas paagutamisel (traditsiooniline meetod kermiste valmistamiseks) on negatiivne mõju materjalidele, mis sisaldavad mangaani – kõrge aururõhuga mangaan hakkab lenduma kõrgetel paagutustemperatuuridel vaakumis ja mangaani kogus materjalis väheneb. Lähtudes mikrostruktuuri analüüsist, röntgen-spektroskoopiast ja röntgenstruktuuranalüüsist ning mehaanilistest katsetest, võib teha järgmised järeldused:

– TiC-FeCr ja TiC-FeCrMn kermiste paagutamine mangaanirikkas atmosfääris mitte ainult ei takista mangaani kadu, vaid võimaldab ka suurendada selle sisaldust paagutatud komposiitides.
– Hoolimata avatud poorsuse olemasolust enne sulafaasi teket, avaldub legeeriv efekt ainult ühe mm paksuses pinnakihis. Legeeriv paagutus ei mõjuta kermiste südamike keemilist koostist ega ka mikrostruktuuri.

Mangaanirikkas keskkonnas avaldab paagutus märkimisväärset mõju titaankarbiidi baasil kermiste pinnakihi mikrostruktuurile ning faasilisele koostisele – eriti kermiste tihenemisele ning mikrostruktuuri ühtlusele, mis omakorda parandab nende mehaanilisi omadusi.